Polymerization of C9 enhances bacterial cell envelope damage and killing by membrane attack complex pores

Dennis J. Doorduijn[1], Dani A.C. Heesterbeek[1], Maartje Ruyken[1], Carla J.C. de Haas[1], Daphne A.C. Stapels[1], Piet C. Aerts[1], Suzan H. M. Rooijakkers[1] and Bart W. Bardoel[1]*

[1] *Department of Medical Microbiology, University Medical Center Utrecht, Utrecht, The Netherlands*

* Corresponding author, e-mail: b.w.bardoel-2@umcutrecht.nl

Abstract

Complement proteins can form Membrane Attack Complex (MAC) pores that directly kill Gram-negative bacteria. MAC pores assemble by stepwise binding of C5b, C6, C7, C8 and finally C9, which can polymerize into a transmembrane ring of up to 18 C9 monomers. It is still unclear if the assembly of a polymeric-C9 ring is necessary to sufficiently damage the bacterial cell envelope to kill bacteria, because a robust way to specifically prevent polymerization of C9 has been lacking. In this paper, polymerization of C9 was prevented without affecting the binding of C9 to C5b-8 by locking the first transmembrane helix domain of C9. We show that polymerization of C9 strongly enhanced bacterial cell envelope damage and killing by MAC pores for several *Escherichia coli* and *Klebsiella* strains. Moreover, we show that polymerization of C9 is impaired on complement-resistant *E. coli* strains that survive killing by MAC pores. Altogether, these insights are important to understand how MAC pores kill bacteria and how bacterial pathogens can resist MAC-dependent killing.

Introduction

Complement proteins in human serum play a crucial role in fighting off invading bacteria. Activation of the complement cascade ultimately results in the assembly of membrane attack complex (MAC) pores that can directly kill Gram-negative bacteria [1–3]. MAC assembly is initiated when recognition molecules, such as antibodies and lectins, bind to bacteria and recruit early complement proteins [4]. This triggers a proteolytic cascade that deposits convertase enzymes on the bacterial surface [5]. These convertases convert complement component C5 into C5b, which initiates the assembly of a large ring-shaped MAC pore that damages the bacterial cell envelope [3,6,7]. Although MAC pores can efficiently kill complement-sensitive bacteria, some bacterial pathogens can survive killing by MAC pores [8–11]. Therefore,

studying how MAC pores kill bacteria is important to understand how the complement system prevents infections and how bacterial pathogens resist killing by MAC pores.

MAC pores assemble in a stepwise manner [12]. When a surface-bound convertase converts C5 into C5b, C5b immediately binds to C6 to form the C5b6 complex [13,14]. Direct binding of C7 to C5b6 stably anchors the MAC precursor to the membrane [15]. Next, C8 binds to membrane-anchored C5b-7, which triggers structural rearrangements in C8 that result in insertion of a transmembrane β-hairpin into the membrane [16,17]. Finally, C9 binds to C5b-8 and polymerizes to form a transmembrane ring of up to 18 monomers C9 with an inner diameter of 11 nm [18,19].

Although C5b-8 can already cause small 1-2 nm lesions in the membrane of erythrocytes and liposomes without a polymeric-C9 ring [17,20], it is still unclear if C9 polymerization is required to sufficiently damage the complex bacterial cell envelope to kill Gram-negative bacteria. On bacteria, MAC pores initially assemble on the outer membrane (OM), which largely consists of lipopolysaccharide (LPS). The O-antigen (O-Ag) of LPS can vary in length between bacterial strains and species [21,22], and this has frequently been associated with complement-resistance [8,9,23,24]. Apart from the OM, the Gram-negative cell envelope also consists of a cytosolic inner membrane (IM) and a periplasmic peptidoglycan layer [25]. We recently developed methods to separately study OM and IM damage in time [14,26]. Here, we wanted to use these methods to study how C9 polymerization contributes to bacterial cell envelope damage by MAC pores. Moreover, a direct causal link between polymerization of C9 and bacterial killing has still not been established, mainly because there was no robust system in which polymerization of C9 could specifically be prevented. Recently, Spicer *et al*. suggested that 'locking' the first transmembrane helix (TMH-1) domain of C9 could prevent polymerization of C9, without affecting the binding of C9 to C5b-8 [27]. Here, we wanted to use this 'locked' C9 to study if C9 polymerization contributes to bacterial cell envelope damage and killing by MAC pores.

In this paper, we show that polymerization of C9 enhanced the efficiency by which MAC pores damage both the OM and IM, which ultimately resulted in faster killing of several *Escherichia coli* and *Klebsiella* strains. This study therefore highlights that MAC pores have to completely assemble to efficiently damage the bacterial cell envelope and kill bacteria. Moreover, we found that polymerization of C9, but not binding of C9 to C5b-8, was impaired on several complement-resistant *E. coli* strains that survive killing by MAC pores. This study therefore also provides insights into how bacterial pathogens resist MAC-dependent killing.

Results

Locking the TMH-1 of C9 strongly impairs its capacity to polymerize, without preventing binding to C5b-8 on *E. coli*

To study the contribution of C9 polymerization to bacterial killing by the MAC, we wanted to use a system in which C9 can bind to C5b-8, but cannot polymerize. Spicer *et al.* recently suggested that the TMH-1 domain of C9 has a crucial role in C9 polymerization [27]. When C9 binds to C5b-8, structural rearrangements in C9 trigger unfurling of the TMH-1 (**Fig. 1a-I**) and TMH-2 (not shown in illustration) to form a transmembrane β-hairpin. Although both TMH domains of C9 insert into the membrane, unfurling of the TMH-1 domain also exposes an elongation surface that allows a subsequent C9 to bind (**Fig. 1a-II**). This ultimately results in the assembly of a polymeric-C9 ring (**Fig. 1a-III**). Based on this crucial role of the TMH-1 domain in polymerization, Spicer *et al.* designed a C9 TMH-1 'lock' mutant ($C9_{TMH\text{-}1\ lock}$) in which the TMH-1 domain was linked to β-strand 4 of the MACPF/CDC domain via an intramolecular cysteine bridge. This lock prevents unfurling of the TMH-1 domain once C9 binds to C5b-8, and thus prevents both the formation of a transmembrane β-hairpin (**Fig. 1a-IV**) and binding of a subsequent C9 (**Fig. 1a-V**). Reducing the cysteine bridge with DTT can unlock the TMH-1 domain and restore its capacity to polymerize (**Fig. 1a-VI**).

$C9_{TMH\text{-}1\ lock}$ was recombinantly expressed and site-specifically labelled with a fluorophore via sortagging, as was done previously for wildtype C9 ($C9_{wt}$) [14]. Fluorescent labelling was comparable between both $C9_{TMH\text{-}1\ lock}$ and $C9_{wt}$ (**S1a**), which means that the fluorescence of both proteins can be directly compared in our assays. $C9_{TMH\text{-}1\ lock}$ showed impaired lysis of sheep erythrocytes compared to $C9_{wt}$, which could be restored by reducing $C9_{TMH\text{-}1\ lock}$ with DTT (**S1b**). Moreover, fluorescent $C9_{TMH\text{-}1\ lock}$ was used to distinguish SDS-stable polymeric-C9 (poly-C9) from monomeric-C9 (mono-C9) by SDS-PAGE, which is frequently used as a read-out for C9 polymerization [28]. $C9_{TMH\text{-}1\ lock}$ did not form poly-C9 together with preassembled C5b6 (pC5b6), C7 and C8, whereas $C9_{wt}$ did (**S1c**). These data confirm that the capacity of $C9_{TMH\text{-}1\ lock}$ to form polymers is impaired, and can be reversed by reducing the cysteine bridge lock.

Next, we wanted to validate that locking the TMH-1 domain only prevents polymerization of C9, without preventing binding of C9 to C5b-8. *E. coli* MG1655 bacteria were incubated in C8-depleted serum to activate complement and label them with MAC precursor C5b-7 (**Fig. 1b**). C5b-7 labelled bacteria were washed to remove remaining serum components and incubated

with C8 and $C9_{wt}$ or $C9_{TMH\text{-}1\ lock}$ to further assemble the MAC. Both $C9_{wt}$ and $C9_{TMH\text{-}1\ lock}$ bound to C5b-7 in a C8-dependent manner as measured by flow cytometry (**Fig. 1c**), although $C9_{wt}$ binding was 10-fold higher than $C9_{TMH\text{-}1\ lock}$. Since the amount of C5b-8 on the surface, as measured by C6-FITC binding, was comparable for both $C9_{wt}$ and $C9_{TMH\text{-}1\ lock}$ (**S1d**), the relative difference in C9 binding suggested a difference in polymerization of C9 (**Fig. 1d**). SDS-PAGE confirmed that only mono-C9 was detected on bacteria incubated with $C9_{TMH\text{-}1\ lock}$ (**Fig. 1e**). Moreover, reducing $C9_{TMH\text{-}1\ lock}$ with DTT increased binding 3-fold compared to $C9_{TMH\text{-}1\ lock}$ without DTT (**Fig. 1c,d**) and resulted in the detection of poly-C9 on bacteria by SDS-PAGE (**Fig. 1e**). This suggests that reducing $C9_{TMH\text{-}1\ lock}$ only partially restored its capacity to polymerize compared to $C9_{wt}$ (**Fig. 1c,d**). Finally, an antibody that recognizes a neo-epitope exposed in poly-C9, which is frequently used for the detection of MAC pores [29], specifically detected bacteria incubated with $C9_{wt}$, but not with $C9_{TMH\text{-}1\ lock}$ (**Fig. 1f**). Altogether, these data indicate that the $C9_{TMH\text{-}1\ lock}$ can bind to C5b-8 on *E. coli*, but that its capacity to polymerize is strongly impaired.

Polymerization of C9 enhances bacterial killing by MAC pores

We then assessed if polymerization of C9 is important for bacterial killing by the MAC. A DNA dye that cannot permeate an intact IM (Sytox) was used to measure the percentage of cells with IM damage by flow cytometry, which we have previously shown to be a sensitive read-out for bacterial killing [14]. Adding $C9_{wt}$ to C5b-8 labelled bacteria resulted in IM damage in a dose-dependent manner, reaching 100% Sytox positive cells from above 3 nM C9 (**Fig. 2a**). For $C9_{TMH\text{-}1\ lock}$, IM damage was impaired and did not increase above 30% Sytox positive cells at 100 nM C9 (**Fig. 2a**). Moreover, bacterial viability was determined by counting colony forming units (CFU's) and decreased only 10-fold for $C9_{TMH\text{-}1\ lock}$ compared to C5b-8 alone, whereas $C9_{wt}$ decreased bacterial viability at least a 1,000-fold (**Fig. 2c**). Reducing $C9_{TMH\text{-}1\ lock}$ with DTT restored its capacity to damage the IM (**Fig. 2b**) and kill bacteria (**Fig. 2c**). Finally, polymerization of $C9_{wt}$ (**Fig. 2d**) and subsequent IM damage (**Fig. 2e**) could be inhibited by $C9_{TMH\text{-}1\ lock}$ in a dose-dependent manner. Poly-C9 detection already decreased by 50% when the amount of $C9_{TMH\text{-}1\ lock}$ was still 10-fold lower than the amount of $C9_{wt}$ (**Fig. 2d**), which suggested that $C9_{TMH\text{-}1\ lock}$ can interfere at multiple stages in the assembly of a polymeric-C9 ring. However, IM damage was only fully inhibited when there was 10-fold more $C9_{TMH\text{-}1\ lock}$ than $C9_{wt}$ (**Fig. 2e**), suggesting that only very few C9 polymers are required to damage the IM. Altogether, our data suggest that polymerization of C9 enhances bacterial killing by MAC pores.

Polymerization of C9 increases OM damage

Since MAC pores initially assemble on the OM [14], we also wondered how C9 polymerization contributes to OM damage. First, OM damage was compared for $C9_{wt}$ and $C9_{TMH\text{-}1\ lock}$ by measuring leakage of periplasmic mCherry ($_{peri}$mCherry, 22 kDa) through the OM of MG1655 using flow cytometry [14]. Adding $C9_{wt}$ to C5b-8 labelled bacteria resulted in rapid leakage of $_{peri}$mCherry within 5 minutes (**Fig. 3a**). By contrast, no more $_{peri}$mCherry leaked out with $C9_{TMH\text{-}1\ lock}$ compared to C5b-8 alone within 60 minutes, suggesting that polymerization of C9 is required to cause leakage of periplasmic proteins through the OM.

We also assessed if C9 polymerization affects the influx of extracellular molecules through the OM. We have previously shown that perturbation of the OM by MAC pores can sensitize Gram-negative bacteria to the antibiotic nisin (3.4 kDa), which normally cannot pass through the OM of Gram-negative bacteria [26]. A 1,000-fold more C5b-8 was required to sensitize bacteria to nisin with $C9_{TMH\text{-}1\ lock}$ compared to $C9_{wt}$ (**Fig. 3b**), suggesting that polymerization of C9 strongly enhanced damage to the OM. Finally, we measured the influx of $DiOC_2$ (0.5 kDa) through the OM in the presence or absence of polymerization. $DiOC_2$ is a green fluorescent dye that shifts to red fluorescence when it is incorporated in membranes with a membrane potential, which in the case of *E. coli* is the IM. With $C9_{TMH\text{-}1\ lock}$, the increase in red:green fluorescence ratio was delayed compared to $C9_{wt}$, suggesting that polymerization of C9 enhanced the influx of $DiOC_2$ through the OM (**Fig. 3c**). When bacteria die the IM potential is lost, which results in a drop of red fluorescence. Loss of IM potential, initiated at the peak in red:green ratio, was also delayed with $C9_{TMH\text{-}1\ lock}$ compared to $C9_{wt}$ (**Fig. 3c**). Interestingly, $C9_{TMH\text{-}1\ lock}$ did cause more rapid influx of $DiOC_2$ (**Fig. 3c**) and nisin (**S2**) through the OM compared to C5b-8 alone. This also suggests that binding of C9 to C5b-8 in the absence of polymerization slightly increases OM damage. Altogether, these data highlight that polymerization of C9 increases damage to the OM.

Polymerization of C9 is rate-limiting in the assembly of complete MAC pores

A recent study suggested that binding of the first C9 to C5b-8 is a kinetic bottleneck in the formation of a complete MAC pore on model lipid membranes [30]. Here, we used $C9_{TMH\text{-}1\ lock}$ to study if this is also the case when MAC pores assemble on bacteria. Therefore, *E. coli* MG1655 were labelled with a constant amount of C5b-8 while the amount of available $C9_{wt}$ and $C9_{TMH\text{-}1\ lock}$ was limited. Binding of $C9_{wt}$ was comparable to $C9_{TMH\text{-}1\ lock}$ when the amount of available C9 was below 1 nM (**Fig. 4a**), suggesting that there is no polymerization when the

amount of available C9 is limited. As the amount of available C9 was increased, binding of $C9_{wt}$ continued to increase up to 10-fold higher than $C9_{TMH\text{-}1\ lock}$ (**Fig. 4a**), whereas binding of $C9_{TMH\text{-}1\ lock}$ saturated (**Fig. 4a**). This suggests that C9 starts polymerizing when all C5b-8 complexes have bound one C9 molecule. This was confirmed by antibody staining (**Fig. 4c**) and SDS-PAGE (**Fig. 4d**), showing mainly mono-C9 when C9 is limited and the appearance of poly-C9 at C9 concentrations above 1 nM. Moreover, when the amount of surface-bound C5b-8 was varied by titrating C8, the difference in $C9_{wt}$ binding compared to $C9_{TMH\text{-}1\ lock}$ binding decreased when an excess of C8 was added (**S3a,b**). $_{peri}$mCherry leakage (**S3c**) and SDS-PAGE (**S3d**) confirmed that an excess of C8 decreased the relative abundance of poly-C9 compared to mono-C9. Altogether, these data suggest that polymerization of C9 is rate-limiting in the assembly of complete MAC pores on bacteria.

Polymerization of C9 enhances bacterial cell envelope damage and killing in serum

So far, we have looked at the effect of C9 polymerization on the MAC in the absence of other serum components. Next, we wanted to see if polymerization of C9 also enhances bacterial cell envelope damage and killing in a serum environment. MG1655 was incubated in 3% C9-depleted serum with $C9_{wt}$ or $C9_{TMH\text{-}1\ lock}$ and influx of $DiOC_2$ or Sytox were measured over time in a plate-reader to measure OM and IM damage respectively. OM damage (**Fig. 5a**) preceded IM damage (**Fig. 5b**), but both were delayed by 30 minutes with $C9_{TMH\text{-}1\ lock}$ compared to $C9_{wt}$. Also, bacterial viability was a 1,000-fold higher for $C9_{TMH\text{-}1\ lock}$ compared to $C9_{wt}$ after 30 minutes (**Fig. 5c**). These data suggest that polymerization of C9 enhances bacterial cell envelope damage and killing in serum.

Interestingly, bacteria were killed with $C9_{TMH\text{-}1\ lock}$ to a comparable level as $C9_{wt}$ after 90 minutes. This was not observed with $C9_{TMH\text{-}1\ lock}$ in the absence of serum (**S4a**), which indicated that the presence of serum affects killing by the MAC, even in the absence of polymerized C9. In serum, complement activation is still ongoing, which could ultimately result in more MAC on the surface of bacteria and explain why viability still decreases in time. Indeed, stopping further MAC formation, by adding C5 conversion inhibitor OmCI after 30 minutes, prevented bacterial killing in C9-depleted serum with $C9_{TMH\text{-}1\ lock}$ over a 100-fold (**Fig. 5c**). Serum also contains bactericidal enzymes that can more efficiently pass through a damaged OM, such as lysozyme (14.7 kDa) and type IIa secreted phospholipase 2A (PLA, 14.5 kDa) [31]. Both lysozyme and PLA decreased bacterial viability when C5b-8 labelled bacteria were incubated with $C9_{TMH\text{-}1\ lock}$ compared to C5b-8 alone (**S4b**), suggesting that these serum proteins also contribute to bacterial killing in serum in the absence of polymerized C9. Nonetheless, taken

together our data mainly highlight that polymerization of C9 enhances the efficiency by which MAC pores damage the bacterial cell envelope and kill bacteria in serum.

Polymerization of C9 enhances cell envelope damage for several *E. coli* and *Klebsiella* strains in serum

We wondered if our findings on *E. coli* MG1655 could also be extrapolated to other *E. coli* strains and other Gram-negative species. First, the effect of C9 polymerization on OM and IM damage was measured for three other complement-sensitive *E. coli* strains (BW25113, MC1061 and 547563.1) in serum. To compare strains, time points were interpolated at which the red:green fluorescence ratio of $DiOC_2$ reached half the value of the peak ($t_{1/2peak}$, shown in **Fig. 5a**) as measure for OM damage, and at which half the maximum Sytox value was reached ($t_{1/2maximum}$, shown in **Fig. 5b**) as measure for IM damage**.** Both OM damage (**Fig. 5d, S5a**) and IM damage (**Fig. 5e, S5b**) were delayed with $C9_{TMH\text{-}1\ lock}$ compared to $C9_{wt}$ for all tested *E. coli* strains. $C9_{TMH\text{-}1\ lock}$ did increase OM damage and IM damage compared to C9-depleted serum alone for three out of four *E. coli* strains (**Fig. 5d,e and S5a,b**). For one strain, 547563.1, $C9_{TMH\text{-}1\ lock}$ only slightly enhanced IM damage, since C9-depleted serum alone already damaged the IM of these bacteria (**Fig. 5e, S5b**). OM damage (**Fig. 5d, S5a**) and IM damage (**Fig 5e, S5b**) were also delayed with $C9_{TMH\text{-}1\ lock}$ compared to $C9_{wt}$ for two clinical *Klebsiella* isolates (*Klebsiella variicola* 402 and *Klebsiella pneumoniae* 567880.1). $C9_{TMH\text{-}1\ lock}$ did not cause IM damage within 90 minutes for *Klebsiella,* suggesting that for *Klebsiella* IM damage by MAC pores was more dependent on polymerization of C9 than for *E. coli*. Altogether, these data suggest that C9 polymerization enhances cell envelope damage for multiple complement-sensitive *E. coli* and *Klebsiella* strains in serum.

Polymerization of C9 is impaired on complement-resistant *E. coli* strains

In our previous study we have identified *E. coli* isolates that survive killing by MAC pores because MAC does not stably insert into the OM [15]. Here, we wanted to see if C9 polymerizes on these complement-resistant *E. coli* strains (clinical isolates 552059.1, 552060.1 and 567705.1). All three complement-resistant strains express LPS O-Ag, whereas only one out of four complement-sensitive strains used in this study did as well (**S6a**). Binding of $C9_{TMH\text{-}1\ lock}$ in 3% C9-depleted serum was comparable between all strains, suggesting that the total amount of C5b-8 on the surface was comparable for complement-sensitive and complement-resistant *E. coli* (**Fig. 6a**)**.** However, for complement-resistant *E. coli* binding of $C9_{wt}$ was similar to $C9_{TMH\text{-}1\ lock}$, suggesting that C9 did not polymerize (**Fig. 6b**). By contrast, binding of $C9_{wt}$ was

5- to 15-fold higher than $C9_{TMH\text{-}1\ lock}$ for all four complement-sensitive *E. coli* (**Fig. 6b**). Adding up to 10-fold more C9 slightly increased the difference between $C9_{wt}$ binding and $C9_{TMH\text{-}1\ lock}$ 2- to 3-fold on complement-resistant 552059.1 (**Fig. 6c**), but this difference was still 5-fold lower compared to complement-sensitive MG1655. Although this suggested that some C9 polymerized on 552059.1, bacteria were still not killed (**S6b**). These data suggest that polymerization of C9, but not binding of C9 to C5b-8, is impaired on complement-resistant *E. coli*.

Finally, our previous study also indicated that although C5b-7 binds to these complement-resistant *E. coli*, it does not properly anchor to the OM [15]. This improper anchoring of C5b-7 ultimately resulted in instable insertion of the MAC, which could be mimicked on complement-sensitive *E. coli* using pC5b6 to assemble MAC [14,15]. In short, MG1655 were labelled with convertases in 10% C5-depleted serum, washed and afterwards pC5b6 was added in combination with C7, C8 and $C9_{wt}$ or $C9_{TMH\text{-}1\ lock}$. For this pC5b6-MAC, $C9_{wt}$ binding was 2- to 3- fold higher compared to $C9_{TMH\text{-}1\ lock}$ (**Fig. 6c**), resembling the difference in binding seen for complement-resistant *E. coli* 552059.1. By contrast, when convertases on MG1655 converted C5 and directly assembled MAC pores (conv-MAC), $C9_{wt}$ binding was 12-fold higher compared to $C9_{TMH\text{-}1\ lock}$ (**Fig. 6c**). Altogether, these data suggest that improper anchoring of C5b-7 results in impaired polymerization of C9 on complement-resistant *E. coli*.

Discussion

Understanding how MAC pores damage the bacterial cell envelope and kill bacteria is important to understand how the complement system prevents infections. Although it was still unclear whether a completely assembled MAC pore is needed to kill bacteria, we here show that it is important to efficiently damage the bacterial cell envelope and rapidly kill multiple Gram-negative bacterial strains and species.

Our findings suggest that bacteria are killed more rapidly when C9 polymerizes, both by MAC alone as well as in a serum environment. Previous reports have already suggested that the absence of C9 delays bacterial killing [32], and have correlated the presence of polymeric-C9 to bacterial killing [33,34]. Our study extends on these insights, since it provides direct evidence that polymerization of C9 enhances bacterial killing by using a system in which C9 can bind to C5b-8 without polymerizing. Although Spicer *et al.* had already suggested that locking the TMH-1 domain of C9 could prevent polymerization of C9, we here validate that this does not affect binding of C9 to C5b-8 [27]. Apart from bacterial killing, our study also suggests that

polymerization of C9 more efficiently damages both the OM and IM of the bacterial cell envelope. Polymerization of C9 greatly enhanced passage of small molecules through the OM and was required for passage of periplasmic proteins through the OM. OM damage preceded IM damage, corresponding with our earlier findings [14]. Here, we add to these insights showing that OM damage also precedes the loss of IM potential, which is a widely accepted characteristic of cell death.

Based on our results, we therefore hypothesize that extensive OM damage by MAC pores is driving bacterial killing. Binding of C8 to C5b-7 allows passage of small molecules through the OM (**Fig 7-I**), but these lesions have minimal effect on the IM and bacterial viability. Binding of C9 to C5b-8 without polymerization of C9 slightly increases damage to both the OM and IM (**Fig 7-II**). Although some residual polymerization of $C9_{TMH\text{-}1\ lock}$ can never be fully excluded, our data do not show any direct evidence that $C9_{TMH\text{-}1\ lock}$ polymerized. Based on the structure of monomeric-C9 [27], it is highly unlikely that the other TMH domain (TMH-2) of C9 can insert into the membrane when the TMH-1 domain is locked. Binding of C9 to C5b-8 without polymerization of C9 could affect the stability by which C8 is inserted into the membrane, which ultimately could affect OM damage. Nonetheless, our data highlight that polymerization of C9 drastically enhanced the damage of both the OM and IM damage and rapidly killed bacteria (**Fig 7-III**). Our study therefore primarily emphasizes that polymerization of C9 strongly enhances bacterial cell envelope damage and killing.

How OM damage by MAC pores destabilizes the IM and kills bacteria remains unclear. The OM is an essential load-bearing membrane that confers stability to the bacterial cell [35]. The extent of OM damage by MAC pores could therefore determine whether a cell can cope with the increase in osmotic pressure. OM damage by MAC pores could even directly interfere with osmoregulation of the cell, as has been suggested for antimicrobial peptides that damage the OM of *E. coli* [36]. Moreover, since metabolism and growth-phase have been associated with sensitivity to killing by MAC pores [37,38], OM damage could also induce a stress response that affects the capacity of a cell to survive envelope stress. C9-depleted serum alone damaged the IM for one *E. coli* strain, even though the amount of C5b-8, indicated by the binding of $C9_{TMH\text{-}1\ lock}$, and OM damage was comparable to other *E. coli* strains. On the other hand, for *Klebsiella* strains IM damage appeared more dependent on polymerization of C9 than for *E. coli* strains. These differences between strains and species could suggest that the capacity of a bacterium to cope with OM damage-related stress is a crucial determinant for bacterial killing

by MAC pores. Further research looking directly at the cellular response of bacteria would be necessary to better understand how OM damage by MAC pores causes cell death.

Our data also suggest that polymerization of C9 is rate-limiting in the assembly of complete MAC pores on bacteria. Joiner *et al*. already demonstrated that limiting the C9 concentration decreased the ratio of C9:C7 on the surface [33]. We further extend on these insights, as our data also suggest that binding of C9 to C5b-8 is favoured over binding to an already unfurled C9 molecule in the nascent polymeric-C9 ring. By contrast, Parsons *et al*. [30] recently suggested that binding of C9 to C5b-8 is a kinetic bottleneck in the assembly of complete MAC pores. However, this study looked at MAC assembly in the presence of an excess of C9, which we here show to affect the assembly kinetics of MAC pores. Moreover, experiments in this study were done on model lipid-membranes that were not labelled with convertases, which also could have influenced the assembly of MAC pores [14].

Finally, our study highlights that polymerization of C9 is specifically impaired on *E. coli* that resist MAC-dependent killing. We have previously shown that C5b-7 could bind to these complement-resistant strains, but was improperly anchored to the OM which resulted in unstably inserted MAC [15]. Here, we extend on these findings showing that this improper anchoring of C5b-7 results in impaired polymerization of C9. How these complement-resistant *E. coli* affect the anchoring of C5b-7 and subsequent polymerization of C9 remains unclear. Polymerization of C9 correlated with the absence of LPS O-Ag in the *E. coli* strains used in this study. The presence and length of LPS O-Ag have been correlated with survival in serum before [23], and are thought to affect the distance of the nascent MAC to the OM and the accessibility of hydrophobic patches in the OM [8]. We therefore hypothesize that improper anchoring of C5b-7 initiates assembly of MAC further away from hydrophobic patches in the OM, which could prevent stable insertion of the nascent polymeric-C9 ring and result in an incomplete polymeric-C9 ring. Although LPS O-Ag modifications can also affect earlier steps in the complement cascade [9,10,39–41], this did not seem to play a role as the amount of C5b-8 on the surface was comparable between complement-sensitive and -resistant *E. coli*. Nonetheless, a more direct study of the effect of O-Ag on polymerization of C9 would be required to verify this hypothesis.

In conclusion, our study provides insight into how MAC pores damage the bacterial cell envelope and kill Gram-negative bacteria. Moreover, our study highlights how bacteria resist killing by MAC pores. These fundamental insights are important to understand how the complement system prevents infections and how bacteria escape killing by the immune system.

Ultimately, these insights may guide the development of future immune therapy against bacteria.

Materials & Methods

Serum and complement proteins

Serum depleted of complement components C5, C8 or C9 was obtained from Complement Technology. Serum was thawed and aliquoted, but not subjected to any further freeze-thaw cycles. Preassembled C5b6 (pC5b6) and C8 were also obtained from Complement Technology. His-tagged complement components C5, C6 and C7 were expressed in HEK293E cells at U-Protein Express as described previously [15]. OmCI was produced in HEK293E cells at U-Protein Express as well and purified as described before [42]. Monoclonal mouse-anti poly-C9 (maE11, kindly provided by T. Mollness and P. Garred) was randomly labelled with NHS-Alexa Fluor AF488 (Thermofisher) according to manufacturer's protocol. Lysozyme was obtained from Raybio and recombinant type IIa secreted phospholipase 2A (PLA) was kindly provided by Gérard Lambeau [43].

Expression and purification of C9

$C9_{wt}$ and $C9_{TMH\text{-}1\ lock}$ (F262C V405C) were cloned into the vector pcDNA34 (Thermo Fisher Scientific) that was modified with an NheI/NotI multiple cloning site. This vector contains a cystatin-S signal peptide and was further modified to encode for the expression of a C-terminal AAA-3x(GGGGS)-LPETGG-HHHHHH tag. gBlocks (Integrated DNA Technologies) containing codon optimized C9 sequences were cloned via Gibson assembly into the NheI/NotI digested pcDNA34 and transformed into Top10F *E. coli*. After verification of the correct sequence, the plasmids were used to transfect EXPI293F cells. EXPI293F cells were grown in EXPI293 medium (Life Technologies) in culture filter cap Erlenmeyer bottles (Corning) on a rotation platform (125 rotations/min) at 37°C, 8% CO_2. One day before transfection, cells were diluted to $2x10^6$ cells/ml. The next day, cells were diluted to $2x10^6$ cells/ml using SFM4Transfx-293 medium, containing UltraGlutamine I (VWR International) prior to transfection using PEI (Polyethylenimine HCl MAX; Polysciences). 0.5 µg DNA/ml cells, containing 50% empty (dummy) vector, was added to Opti-MEM (1:10 of total volume; Gibco) and gently mixed. After adding 1 µg/ml PEI in a PEI/DNA (w/w) ratio of 5:1, the mixture was incubated at room temperature for 20 min and added dropwise to cells while manually rotating the culture flask. After 3.5 hours, 1 mM valproic acid (Sigma) was added. After 5 days of

expression, the cell supernatant was collected by centrifugation and filtration (0.45 µm). Cell supernatant was diafiltrated over a 30 kDa membrane on a Quixstand (GE healthcare) to Tris/NaCl buffer (50 mM Tris/500 mM NaCl at pH 8.0). Proteins were finally loaded on a HisTrap HP Chelating column (GE healthcare) in Tris/NaCl buffer supplemented with 40 mM imidazole and eluted with 150 mM imidazole. Final purification was done by size-exclusion chromatography (SEC) on a Superdex 200 Increase column (GE Healthcare) on an Akta Explorer (GE Healthcare) with PBS. The concentration of proteins was determined by measuring absorbance at 280 nm and verified by SDS-PAGE.

Site-specific fluorescent labelling of MAC components

C6 and C9 were labelled with fluorescent probes as described previously [14,15]. 50 µM of protein with C-terminal LPETGG-His tag was incubated with 25 µM His-tagged sortase-A7+ [44] and 1 mM GGG-substrate in Tris/NaCl buffer (50 mM Tris/300 mM NaCl at pH 7.8) for two hours at 4 °C. GGGK-FITC (Isogen Life Science) was used for C6-LPETGG-His and GGGK-azide (Genscript) for C9-LPETGG-His. Sortagged proteins were purified on a HisTrap FF column (GE Healthcare), which captures protein that was not sortagged and still contains a His-tag. FITC-labelled C6 was directly purified by SEC on a Superdex 200 Increase column on the Akta Explorer with PBS. GGG-azide labelled proteins were concentrated to 25 µM on a 30 kDa Amicon Tube (Merck Millipore) in Tris/NaCl buffer and next labelled with 100 µM DBCO-Cy5 (Sigma Aldrich) via copper-free click chemistry for 3h at 4 °C. Finally, Cy5-labelled proteins were also purified by SEC on a Superdex 200 Increase column with PBS. Labelling of the proteins was monitored during SEC by measuring absorbance at 280 nm (protein), 488 nm (FITC) and 633 nm (Cy5) nm and finally verified by SDS-PAGE by measuring in-gel fluorescence with LAS4000 Imagequant (GE Healthcare).

Bacterial strains

Unless otherwise specified, the common laboratory *E. coli* strain MG1655 was used in our experiments. For experiments where leakage of periplasmic mCherry was measured, MG1655 was used transformed with pPerimCh containing a constitutively expressed periplasmic mCherry ($_{peri}$mCherry) previously used in [14]. Other laboratory *E. coli* strains that were used in this study included BW25113 and MC1061. Clinical isolates, namely *E. coli* 547563.1, 552059.1, 552060.1, 567705.1, *Klebsiella variicola* 402 and *Klebsiella pneumonia*e 567880.1, were obtained from the clinical Medical Microbiology department at the University Medical Center Utrecht.

Bacterial growth

For all experiments, bacteria were plated on Lysogeny Broth (LB) agar plates. Single colonies were picked and grown overnight at 37 °C in LB medium. For MG1655 transformed with pPerimCh, LB was supplemented with 100 µg/ml ampicillin. The next day, subcultures were grown by diluting at least 1/30 and these were grown to mid-log phase (OD600 between 0.4 – 0.6). Once grown to mid-log phase, bacteria were washed by centrifugation three times (11000 rcf for 2 minutes) and resuspended to OD 1.0 (~1 x 10^9 bacteria/ml) in RPMI (Gibco) + 0.05% human serum albumin (HSA, Sanquin).

Complement labelling and serum bactericidal assays

For MAC-specific bactericidal assays, bacteria were labelled with C5b-7 as described previously [15]. In short, bacteria (~1 x 10^8 bacteria/ml) were incubated with 10 % C8-depleted serum for 30 minutes at 37 °C, washed three times and resuspended in RPMI-HSA. C5b-7 labelled bacteria (~5 x 10^7 bacteria/ml) were incubated for 30 minutes at 37 °C with 10 nM C8 and 20 nM C9, unless stated differently. When C9 was reduced with 10 mM dithiothreitol (DTT), 20 nM C8 was added to bacteria (~5 x 10^7 bacteria/ml) 15 minutes at RT before C9 was added to allow binding of C8 to C5b-7. To label bacteria with convertases, bacteria (~1 x 10^8 bacteria/ml) were incubated with 10 % C5-depleted serum for 30 minutes at 37 °C as described previously [14,15]. Washing steps were done by pelleting bacteria at 11,000 rcf for 2 minutes and washing with RPMI-HSA. For serum bactericidal assays, bacteria (~5 x 10^7 bacteria/ml) were incubated with 3% C9-depleted serum supplemented with physiological concentrations of C9 (100% serum ± 1 µM) for 30 minutes at 37 °C, unless stated differently. KP880.1 was incubated in 10% C9-depleted serum with the corresponding physiological concentration of C9. Blocking of C5 conversion in serum was done with 25 µg/ml OmCI as final concentration. For assays where nisin (Handary, SA, Brussels) was added, 3 µg/ml was used as final concentration.

Flow cytometry

Complement-labelled bacteria (~5 x 10^7 bacteria/ml) were incubated with 2.5 µM of Sytox Blue Dead Cell stain (Thermofisher). Samples were diluted to ~2.5 x 10^6 bacteria/ml in RPMI-HSA and subsequently analyzed on a MACSquant VYB (Miltenyi Biotech) for Sytox and $_{peri}$mCherry fluorescence. Poly-C9 deposition was measured by incubating bacteria (2.5 x 10^7 bacteria/ml) with 6 µg/ml monoclonal AF488 labelled mouse-anti poly-C9 (maE11) for 30 minutes at 4 °C. For C9 binding in serum, bacteria were stained with 1 µM Syto9 (Thermofisher) to exclude serum noise events. Samples were next diluted to ~2.5 x 10^6

bacteria/ml in 1.1% paraformaldehyde and subsequently analyzed on the BD FACSVerse flow cytometer for Cy5 and maE11-AF488 or Syto9 fluorescence. Flow cytometry data was analysed in FlowJo V.10. Bacteria were gated on forward scatter and side scatter. In serum, an additional trigger was placed on Syto9 fluorescence. Sytox positive cells were gated such that the buffer only control had <1 % positive cells.

Poly-C9 detection by SDS-PAGE

Bacterial labelled with complement components were collected by spinning bacteria down 11,000 rcf for 2 minutes and subsequently washing cell pellets twice in RPMI-HSA. Cell pellets were resuspended and diluted 1:1 in SDS sample buffer (0.1M Tris (pH 6.8), 39% glycerol, 0.6% SDS and bromophenol blue) supplemented with 50 mg/ml DTT and placed at 95 °C for 5 minutes. Samples were run on a 4-12% Bis-Tris gradient gel (Invitrogen) for 75 minutes at 200V. Gels were imaged for 10 minutes with increments of 30 seconds on the LAS4000 Imagequant (GE Healthcare) for in-gel Cy5 fluorescence. Monomeric-C9 (mono-C9) and polymeric-C9 (poly-C9) were distinguished by size, since mono-C9 runs at 63 kDa and poly-C9 is retained in the comb of the gel.

Bacterial viability assay

Bacteria were treated with MAC components or serum as described above. Next, colony forming units (CFU) were determined by making serial dilutions in PBS (100, 1.000, 10.000 and 100.000-fold). Serial dilutions were plated in duplicate on LB agar plates and incubated overnight at 37 °C. The next day, colonies were counted and the corresponding concentration of CFU/ml was calculated.

Multi-well fluorescence assays

Bacteria (~5 x 10^7 bacteria/ml) added to RPMI-HSA supplemented with 1 µM of Sytox Green Dead Cell stain (Thermofisher) or 30 µM $DiOC_2$ (PromoCell). Bacteria were next incubated with MAC components, serum and/or nisin as described above. Fluorescence was measured every 60 seconds on a Clariostar platereader (BMG labtech). Sytox green fluorescence was measured using an excitation wavelength of 484-15 nm and emission wavelength of 527-20. $DiOC_2$ fluorescence was measured using an excitation wavelength 484-15 nm and emission wavelength of 527-20 (green) and 650-24 (red). For $DiOC_2$, the red fluorescence was divided by the green fluorescence to determine the red:green fluorescence ratio. $t_{1/2peak}$ for $DiOC_2$ was

interpolated at half the value of the peak, which was calculated by substracting the background ratio value at t=0 from the peak ratio value and dividing by two. $t_{1/2maximum}$ for Sytox was interpolated at half the value of the maximum Sytox value, which was calculated by substracting the fluorescence value at t=0 from the maximum fluorescence value and dividing by two.

LPS O-antigen Silver staining

E. coli strains were typed for LPS O-Ag by Silver staining after SDS-PAGE based on [45,46]. In short, bacteria were scraped from blood agars plates in PBS and incubated at 56 °C for 60 minutes. Cell pellets were next deproteinated with 400 µg/ml proteinase K for 90 minutes and diluted in 2x Laemli buffer with 0.7 M beta-mercaptoethanol. Cell pellets were run on a 4-12% BisTris gel as described above and fixed overnight in fixing buffer (40% ethanol + 4% glacial acetic acid). The gel was oxidized for 5 minutes in fixing buffer supplemented with 0.6% periodic acid. The gel was then stained for 15 minutes with freshly prepared 0.3% silver nitrate in 0.125 M sodium hydroxide and 0.3% ammonium hydroxide. Finally, the gel was developed for 7 minutes in developer solution (0.25% citric acid + and 0.2% formaldehyde). In between steps, the gel was washed three times with MilliQ. Lipid A and LPS core were distinguished from LPS O-Ag based on size.

Data analysis and statistical testing

Unless stated otherwise, graphs are comprised of at least three biological replicates. Statistical analyses were performed in GraphPad Prism 8 and are further specified in the figure legends.

Acknowledgements

This work was funded by an ERC Starting grant (639209-ComBact, to S.H.M.R). The authors would like to acknowledge Lisanne de Vor and Myrthe Reiche for critically reading the manuscript.

Author contributions

D.J.D., S.H.M. and B.W.B. conceived the project and designed the experiments. D.J.D. and C.J.C.H. performed protein purifications and fluorescent labelling. D.J.D. performed poly-C9 detection by SDS-PAGE. D.J.D., D.A.C.H., M.R. and B.W.B. performed flow cytometry, multiwell fluorescence and bacterial killing assays. P.C.A. performed LPS O-Ag typing with input from D.A.C.S. D.J.D., D.A.C.H., M.R., D.A.C.S., S.H.M., B.W.B. analyzed the data.

D.J.D., S.H.M. and B.W.B. wrote the manuscript with input from D.A.C.H., D.A.C.S. All authors approved the final version of the manuscript.

Competing interests

The authors declare no competing interests.

References

1. Taylor PW. Bactericidal and bacteriolytic activity of serum against gram-negative bacteria. Microbiol Rev. 1983;47(1):46–83.

2. Joiner KA, Brown EJ, Frank MM. Complement and bacteria. Annu Rev Immunol. 1984;2:461–91.

3. Doorduijn DJ, Rooijakkers SHM, Heesterbeek DAC. How the Membrane Attack Complex Damages the Bacterial Cell Envelope and Kills Gram-Negative Bacteria. Bioessays. 2019;41(10):e1900074.

4. Gasque P. Complement: A unique innate immune sensor for danger signals. Mol Immunol. 2004;41(11 SPEC. ISS.):1089–98.

5. Merle NS, Church SE, Fremeaux-Bacchi V, Roumenina LT. Complement system part I - molecular mechanisms of activation and regulation. Front Immunol. 2015;6(JUN):1–30.

6. Bhakdi S, Tranum-Jensen J. Molecular nature of the complement lesion. Proc Natl Acad Sci U S A. 1978;75(11):5655–9.

7. Müller-Eberhard HJ. The membrane attack complex of complement. Annu Rev Immunol. 1986;4:503–28.

8. Joiner KA. Complement evasion by bacteria and parasites. Annu Rev Microbiol. 1988 May;42(4):201–30.

9. Merino S, Camprubi S, Alberti S, Benedi VJ, Tomas JM. Mechanisms of *Klebsiella pneumoniae* resistance to complement-mediated killing. Infect Immun. 1992;60(6):2529–35.

10. Doorduijn DJ, Rooijakkers SHM, van Schaik W, Bardoel BW. Complement resistance mechanisms of *Klebsiella pneumoniae*. Immunobiology. 2016 Oct;221(10):1102–9.

509 11. Abreu AG, Barbosa AS. How *Escherichia coli* Circumvent Complement-Mediated
510 Killing. Front Immunol. 2017;8(April):1–6.

511 12. Bayly-Jones C, Bubeck D, Dunstone MA. The mystery behind membrane insertion: A
512 review of the complement membrane attack complex. Philos Trans R Soc B Biol Sci.
513 2017;372(1726).

514 13. DiScipio RG, Linton SM, Rushmere NK. Function of the factor I modules (FIMS) of
515 human complement component C6. J Biol Chem. 1999;274(45):31811–8.

516 14. Heesterbeek DA, Bardoel BW, Parsons ES, Bennett I, Ruyken M, Doorduijn DJ, et al.
517 Bacterial killing by complement requires membrane attack complex formation via
518 surface-bound C5 convertases. EMBO J. 2019 Feb 15;38(4):1–17.

519 15. Doorduijn DJ, Bardoel BW, Heesterbeek DAC, Ruyken M, Benn G, Parsons ES, et al.
520 Bacterial killing by complement requires direct anchoring of membrane attack complex
521 precursor C5b-7. PLoS Pathog. 2020;16(6 June):1–23.

522 16. Brannen CL, Sodetz JM. Incorporation of human complement C8 into the membrane
523 attack complex is mediated by a binding site located within the C8beta MACPF domain.
524 Mol Immunol. 2007;44(5):960–5.

525 17. Sharp TH, Koster AJ, Gros P. Heterogeneous MAC Initiator and Pore Structures in a
526 Lipid Bilayer by Phase-Plate Cryo-electron Tomography. Cell Rep. 2016;15(1):1–8.

527 18. Serna M, Giles JL, Morgan BP, Bubeck D. Structural basis of complement membrane
528 attack complex formation. Nat Commun. 2016;7:10587.

529 19. Menny A, Serna M, Boyd CM, Gardner S, Praveen Joseph A, Paul Morgan B, et al.
530 CryoEM reveals how the complement membrane attack complex ruptures lipid bilayers.
531 Nat Commun. 2018;(2018):1–11.

532 20. Bhakdi S, Tranum-Jensen J. C5b-9 assembly: Average binding of one C9 molecule to
533 C5b-8 without poly-C9 formation generates a stable transmembrane pore. J Immunol.
534 1986;136(8):2999–3005.

535 21. Wang L, Wang Q, Reeves PR. The Variation of O Antigens in Gram-Negative Bacteria.
536 In: Biochemistry. 2010. p. 123–52.

537 22. Liu B, Furevi A, Perepelov A V., Guo X, Cao H, Wang Q, et al. Structure and genetics

538 of Escherichia coli O antigens. FEMS Microbiol Rev. 2020;44(6):655–83.

539 23. Grossman N, Schmetz MA, Foulds J, Klima EN, Jimenez-Lucho VE, Leive LL, et al.
540 Lipopolysaccharide size and distribution determine serum resistance in S*almonella*
541 *montevideo*. J Bacteriol. 1987;169(2):856–63.

542 24. Miglioli PA, Toni M. Serum sensitivity of *Escherichia coli* strains present in the clinical
543 environment. J Chemother. 1989 Jun;1(3):162–3.

544 25. Silhavy TJ, Kahne D, Walker S. The bacterial cell envelope. Cold Spring Harb Perspect
545 Biol. 2010;2(5):a000414.

546 26. Heesterbeek DAC, Martin NI, Velthuizen A, Duijst M, Ruyken M, Wubbolts R, et al.
547 Complement-dependent outer membrane perturbation sensitizes Gram-negative bacteria
548 to Gram-positive specific antibiotics. Sci Rep. 2019;9(1):1–10.

549 27. Spicer BA, Law RHP, Caradoc-Davies TT, Ekkel SM, Bayly-Jones C, Pang S-S, et al.
550 The first transmembrane region of complement component-9 acts as a brake on its self-
551 assembly. Nat Commun. 2018 Dec 15;9(1):3266.

552 28. Podack ER, Tschopp J. Circular polymerization of the ninth component of complement.
553 Ring closure of the tubular complex confers resistance to detergent dissociation and to
554 proteolytic degradation. J Biol Chem. 1982;257(24):15204–12.

555 29. Mollnes TE, Lea T, Frøland SS, Harboe M. Quantification of the terminal complement
556 complex in human plasma by an enzyme-linked immunosorbent assay based on
557 monoclonal antibodies against a neoantigen of the complex. Scand J Immunol. 1985
558 Aug;22(2):197–202.

559 30. Parsons ES, Stanley GJ, Pyne ALB, Hodel AW, Nievergelt AP, Menny A, et al. Single-
560 molecule kinetics of pore assembly by the membrane attack complex. Nat Commun.
561 2019;10(1):472274.

562 31. Heesterbeek DAC, Muts RM, van Hensbergen VP, de Saint Aulaire P, Wennekes T,
563 Bardoel BW, et al. Outer membrane permeabilization by the membrane attack complex
564 sensitizes Gram-negative bacteria to antimicrobial proteins in serum and phagocytes.
565 PLoS Pathog. 2021;17(1):1–22.

566 32. Harriman GR, Esser AF, Podack ER, Wunderlich AC, Braude AI, Lint TF, et al. The
567 role of C9 in complement-mediated killing of *Neisseria*. J Immunol. 1981

568 Dec;127(6):2386–90.

569 33. Joiner KA, Schmetz MA, Sanders ME, Murray TG, Hammer CH, Dourmashkin R, et al.
570 Multimeric complement component C9 is necessary for killing of *Escherichia coli* J5 by
571 terminal attack complex C5b-9. Proc Natl Acad Sci U S A. 1985;82(14):4808–12.

572 34. Bloch EF, Schmetz MA, Foulds J, Hammer CH, Frank MM, Joiner KA. Multimeric C9
573 within C5b-9 is required for inner membrane damage to *Escherichia coli* J5 during
574 complement killing. J Immunol. 1987;138(3):842–8.

575 35. Rojas ER, Billings G, Odermatt PD, Auer GK, Zhu L, Miguel A, et al. The outer
576 membrane is an essential load-bearing element in Gram-negative bacteria. Nature.
577 2018;559(7715):617–21.

578 36. Hartmann M, Berditsch M, Hawecker J, Ardakani MF, Gerthsen D, Ulrich AS. Damage
579 of the bacterial cell envelope by antimicrobial peptides gramicidin S and PGLa as
580 revealed by transmission and scanning electron microscopy. Antimicrob Agents
581 Chemother. 2010;54(8):3132–42.

582 37. Taylor PW, Kroll HP. Killing of an encapsulated strain of *Escherichia coli* by human
583 serum. Infect Immun. 1983;39(1):122–31.

584 38. Barnes MG, Weiss AA. Growth phase influences complement resistance of *Bordetella*
585 *pertussis*. Infect Immun. 2002;70(1):403–6.

586 39. Sansano M, Reynard AM, Cunningham RK. Inhibition of serum bactericidal reaction by
587 lipopolysaccharide. Infect Immun. 1985;48(3):759–62.

588 40. Bravo D, Silva C, Carter JA, Hoare A, Alvarez SA, Blondel CJ, et al. Growth-phase
589 regulation of lipopolysaccharide O-antigen chain length influences serum resistance in
590 serovars of *Salmonella*. J Med Microbiol. 2008 Aug 1;57(8):938–46.

591 41. Miajlovic H, Smith SG. Bacterial self-defence: How *Escherichia coli* evades serum
592 killing. FEMS Microbiol Lett. 2014;354(1):1–9.

593 42. Nunn M a, Sharma A, Paesen GC, Adamson S, Lissina O, Willis AC, et al. Complement
594 inhibitor of C5 activation from the soft tick *Ornithodoros moubata*. J Immunol.
595 2005;174(4):2084–91.

596 43. Ghomashchi F, Brglez V, Payré C, Jeammet L, Bezzine S, Gelb MH, et al. Preparation

of the Full Set of Recombinant Mouse- and Human-Secreted Phospholipases A2. 1st ed. Vol. 583, Methods in Enzymology. Elsevier Inc.; 2017. 35–69 p.

44. Jeong HJ, Abhiraman GC, Story CM, Ingram JR, Dougan SK. Generation of Ca2+-independent sortase A mutants with enhanced activity for protein and cell surface labeling. PLoS One. 2017;12(12):1–15.

45. Hitchcock PJ, Brown TM. Morphological heterogeneity among *Salmonella* lipopolysaccharide chemotypes in silver-stained polyacrylamide gels. J Bacteriol. 1983;154(1):269–77.

46. Chart H. Lipopolysaccharide chemotyping. Methods Mol Biol. 1995;46:41–8.

Figure 1 – $C9_{TMH\text{-}1\ lock}$ binds to C5b-8, but its capacity to form polymers is impaired on *E. coli*

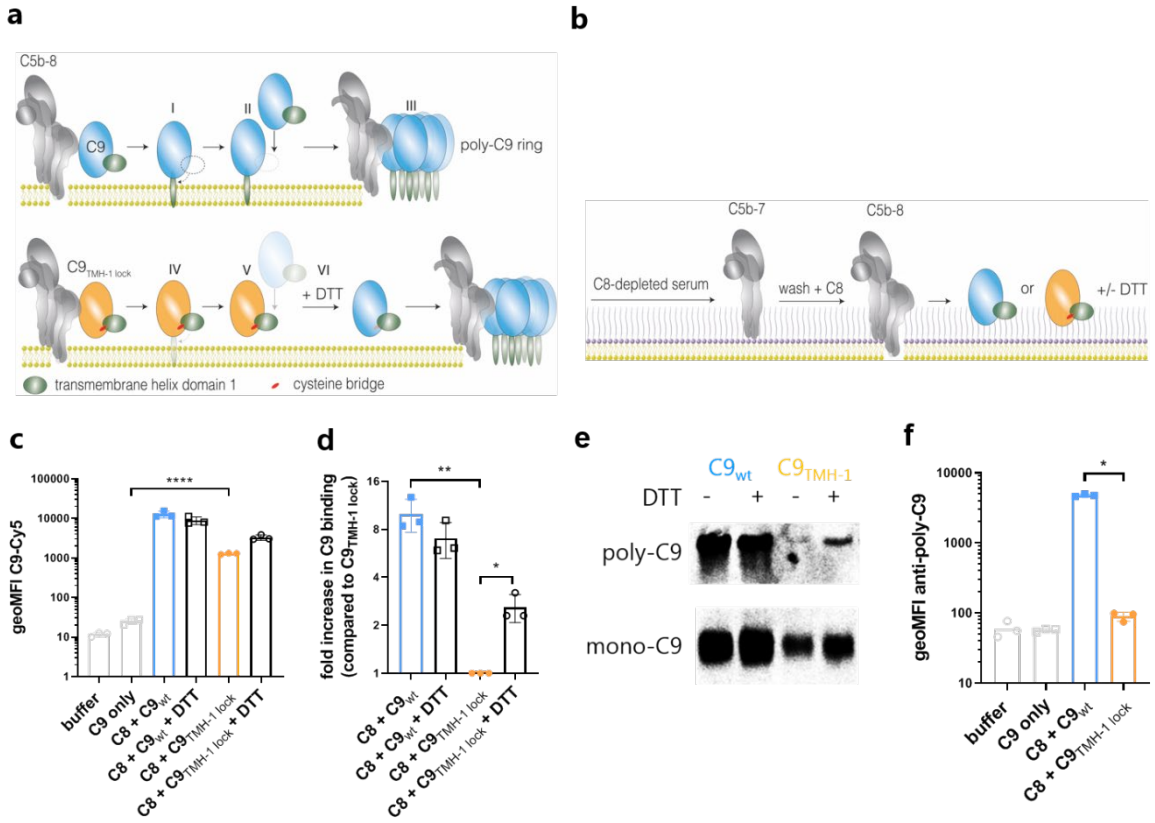

a) Schematic overview of C9 polymerization. Binding of C9 (blue) to C5b-8 (grey) triggers unfurling of the TMH-1 domain of C9 (green) and subsequent insertion into the membrane (I). Unfurling of TMH-1 exposes the elongation surface of C9 to bind a subsequent C9 monomer (II). Ultimately, this results in the formation of a C9 polymer (III). Locking the TMH-1 domain of C9 (orange, $C9_{TMH\text{-}1\ lock}$) with an intramolecular cysteine bridge (red) prevents unfurling of the TMH-1 domain when C9 binds to C5b-8 (IV). This also prevents exposure of the elongation surface of $C9_{TMH\text{-}1\ lock}$ and subsequent polymerization (V). Reducing the cysteine bridge of $C9_{TMH\text{-}1\ lock}$ with DTT restores its capacity to form polymers (VI). b) Schematic overview of labelling *E. coli* MG1655 with MAC. *E. coli* is labelled with C5b-7 by incubating them in 10% C8-depleted serum for 30 minutes. Bacteria are washed and next incubated with 10 nM C8 for 15 minutes. Finally, 20 nM of Cy5-labelled $C9_{wt}$ or $C9_{TMH\text{-}1\ lock}$ is added in the presence or absence of 10 mM DTT for 30 minutes to measure C9 binding. c) Binding of Cy5-labelled $C9_{wt}$ or $C9_{TMH\text{-}1\ lock}$ to bacteria treated as described in b and measured by flow cytometry. d) Binding of Cy5-labelled C9 in c was divided by the fluorescence of bacteria labelled with C8 + $C9_{TMH\text{-}1\ lock}$ to calculate the relative binding difference as indication for polymerization of C9. e)

626 Bacterial cell pellets were analyzed by SDS-PAGE for in-gel fluorescence of Cy5-labelled $C9_{wt}$
627 or $C9_{TMH\text{-}1\ lock}$ to distinguish monomeric-C9 (mono-C9) from polymeric-C9 (poly-C9). f)
628 Bacteria were stained with AF488-labelled mouse anti-poly-C9 aE11-antibody and staining
629 was measured by flow cytometry. Flow cytometry data are represented by individual geoMFI
630 values of the bacterial population. SDS-PAGE images are representative for at least three
631 independent experiments. Data represent individual values of three independent experiments
632 with mean +/- SD. Statistical analysis was done on log-transformed data (^{10}log for c, f and ^{2}log
633 for d) using a paired one-way ANOVA with Tukey's multiple comparisons' test. Significance
634 was shown as * $p \leq 0.05$, ** $p \leq 0.005$, **** $p \leq 0.0001$.

635

Figure 2 – Polymerization of C9 enhances bacterial killing by MAC pores

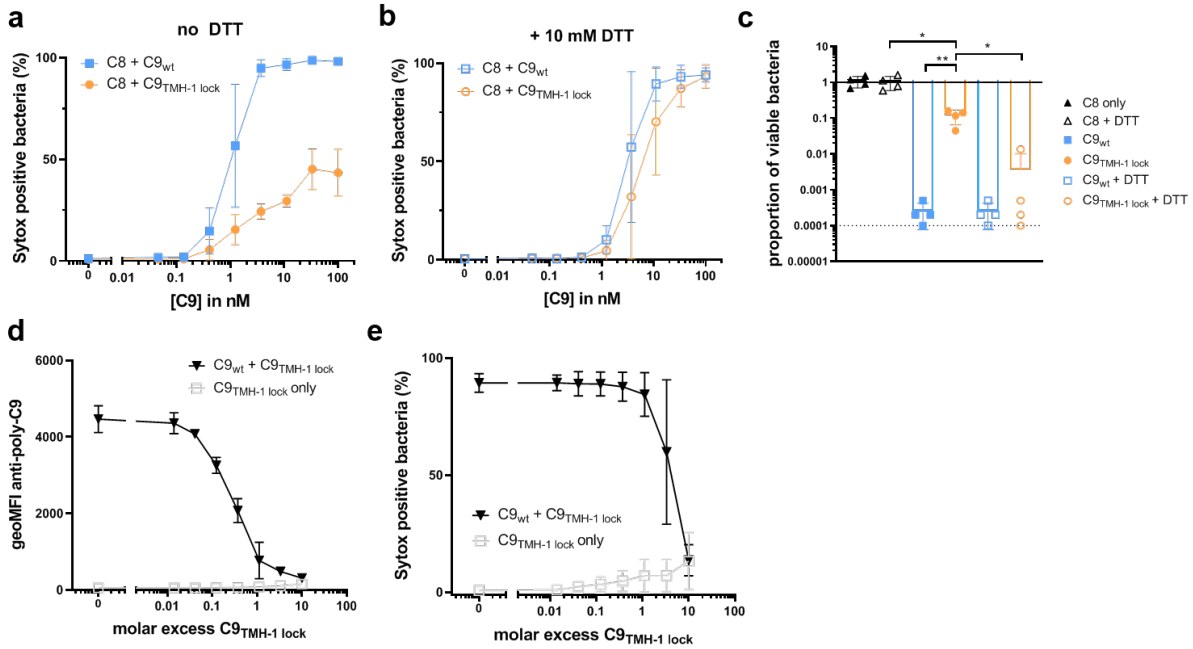

E. coli MG1655 were labelled with C5b-7 by incubating them in 10% C8-depleted serum for 30 minutes. Bacteria were washed and next incubated with 10 nM C8 for 15 minutes. a-c) A concentration range of $C9_{wt}$ or $C9_{TMH\text{-}1\ lock}$ was added in the absence (a) or presence (b) of 10 mM DTT for 30 minutes. Sytox was used to determine the percentage of cells that have a damaged bacterial IM by flow cytometry as read-out for bacterial killing. c) At 100 nM C9, bacterial viability was determined by counting colony forming units (CFU's) and calculating the proportion of viable cells compared to C5b-7 labelled bacteria in buffer. The horizontal dotted line represents the detection limit of the assay. d-e) C5b-8 labelled bacteria were incubated for 30 minutes with 20 nM $C9_{wt}$ and a concentration range of $C9_{TMH\text{-}1\ lock}$. Bacteria were stained with AF488-labelled mouse anti-poly-C9 aE11-antibody (d) and Sytox to determine the percentage of cells that has a damaged bacterial IM (e) by flow cytometry. Flow cytometry data are represented by geoMFI values or cell frequencies of the bacterial population. Data represent mean values +/- SD (a,b,d,e) or individual values (c) of three independent experiments with mean +/- SD. Statistical analysis was done on ^{10}log-transformed data (c) using a paired one-way ANOVA with Tukey's multiple comparisons' test. Significance was shown as * $p \leq 0.05$, ** $p \leq 0.005$.

Figure 3 – Polymerization of C9 increases OM damage by MAC pores

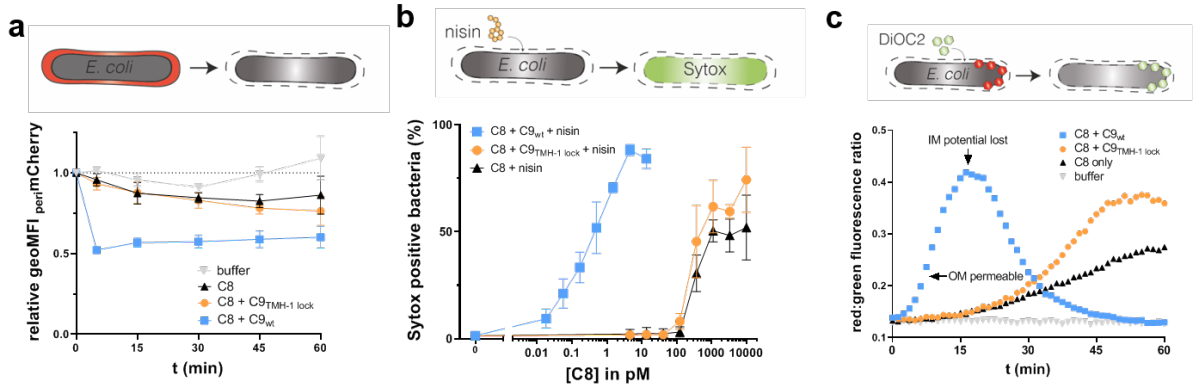

E. coli MG1655 were labelled with C5b-7 by incubating them in 10% C8-depleted serum for 30 minutes. Bacteria were washed and next incubated with buffer, 10 nM C8 with 20 nM $C9_{wt}$ or $C9_{TMH\text{-}1\ lock}$ to measure damage to the bacterial OM. a) periplasmic mCherry ($_{peri}$mCherry, red) leakage was measured at different time points by flow cytometry and represented as relative $_{peri}$mCherry fluorescence compared to t=0. b) C5b-7 labelled bacteria were incubated with a concentration range of C8 and 20 nM $C9_{wt}$ or $C9_{TMH\text{-}1\ lock}$ supplemented with 3 µg/ml nisin for 30 minutes. Nisin influx through OM was measured using Sytox to determine the percentage of cells that have a damaged bacterial IM as read-out for bacterial killing by flow cytometry after 30 minutes. c) $DiOC_2$ enters the cells when the OM is permeable and shifts from green to red fluorescence in cells with an intact inner membrane (IM) potential. $DiOC_2$ shifts back to green fluorescence when the IM potential is lost. Flow cytometry data are represented by geoMFI values of the bacterial population. Data represent mean +/- SD of three independent experiments. Multiwell plate-reader assays are shown by one representative experiment that has been repeated at least three times.

672 **Figure 4 – Polymerization of C9 is rate-limiting in the assembly of a complete MAC pore**

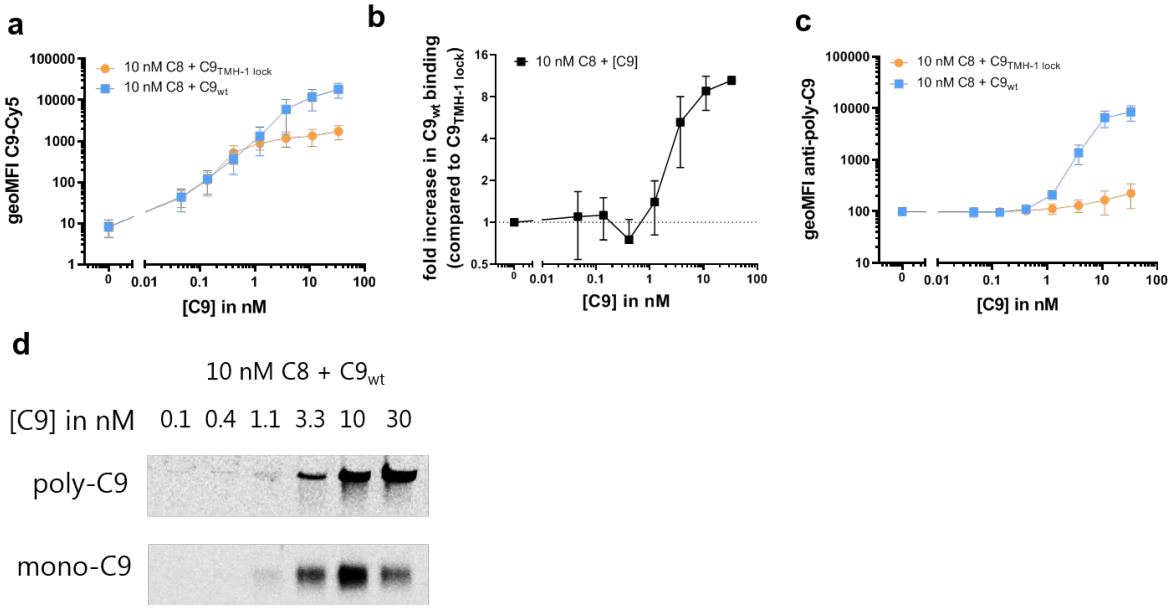

673

674 *E. coli* MG1655 were labelled with C5b-7 by incubating them in 10% C8-depleted serum for
675 30 minutes. Bacteria were washed and next incubated with 10 nM C8 and a concentration range
676 of Cy5-labelled $C9_{wt}$ or $C9_{TMH\text{-}1\ lock}$ for 30 minutes to measure binding of C9. a) Binding of
677 Cy5-labelled $C9_{wt}$ or $C9_{TMH\text{-}1\ lock}$ to bacteria measured by flow cytometry. b) The relative
678 increase in $C9_{wt}$ binding compared to bacteria labelled with $C9_{TMH\text{-}1\ lock}$ was calculated as
679 indication for C9 polymerization. c) Bacteria were stained with AF488-labelled mouse anti-
680 poly-C9 aE11-antibody and staining was measured by flow cytometry. d) Bacterial cell pellets
681 were analyzed by SDS-PAGE for in-gel fluorescence of Cy5-labelled $C9_{wt}$ to distinguish
682 monomeric-C9 (mono-C9) from polymeric-C9 (poly-C9). Flow cytometry data are represented
683 by geoMFI values of the bacterial population. Data represent mean +/- SD of three independent
684 experiments. SDS-PAGE images are representative for at least three independent experiments.

685

686 **Figure 5 – Polymerization of C9 enhances bacterial cell envelope damage and killing in**
687 **serum**

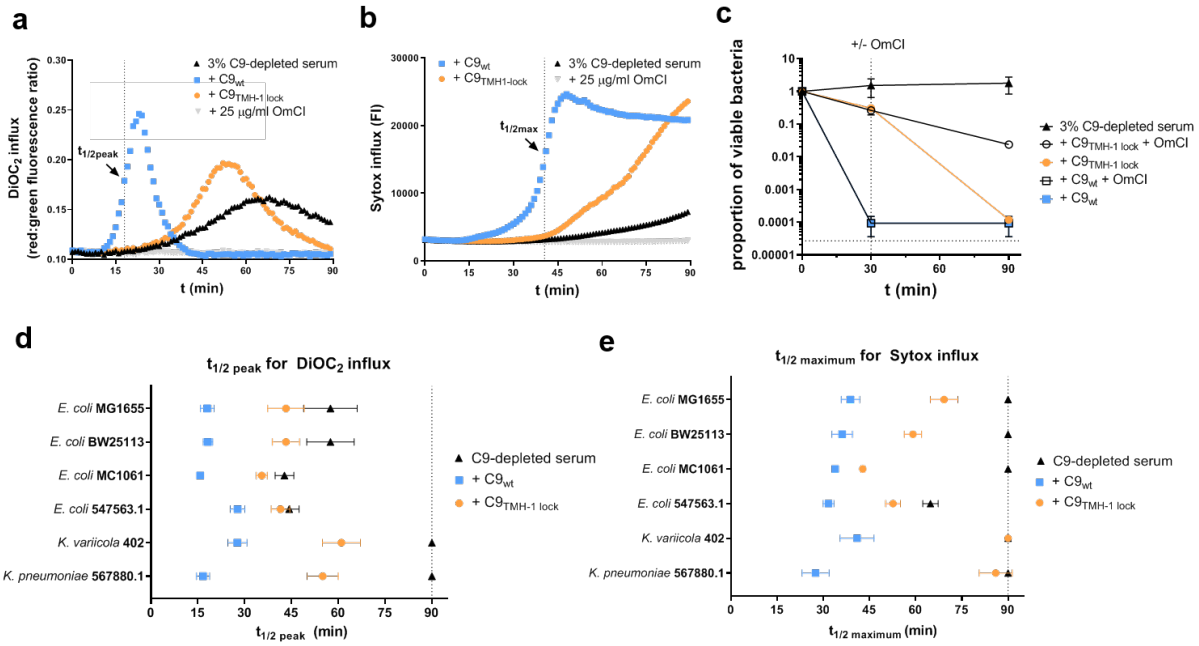

688

689 *E. coli* MG1655 were incubated in 3% C9-depleted serum supplemented with a physiological
690 concentration (= 25 nM) of $C9_{wt}$ or $C9_{TMH\text{-}1\ lock}$ for 90 minutes. As negative control, 25 µg/ml
691 C5 conversion inhibitor OmCI was added to the serum. a) OM damage was measured by $DiOC_2$
692 influx, which was determined by the shift in red:green fluorescence ratio over time in a
693 multiwell plate-reader assay. b) IM damage was measured by Sytox influx over time in a
694 multiwell plate-reader assay. c) Bacterial viability was determined at different time points by
695 counting colony forming units (CFU's) and calculating the proportion of viable cells compared
696 to t=0. At t=30 (vertical dotted line), buffer was added (closed symbols) or OmCI (open
697 symbols) to stop MAC formation. The horizontal dotted line represents the detection limit of
698 the assay. d-e) Other *E. coli* strains (BW25113, MC1061, 547563.1) and *K. variicola* 402 were
699 also incubated in 3% C9-depleted serum supplemented with $C9_{wt}$ or $C9_{TMH\text{-}1\ lock}$ for 90 minutes.
700 *K. pneumoniae* 567880.1 was incubated in 10% C9-depleted serum because of less efficient
701 activation of the complement cascade and was therefore also supplemented with 80 nM $C9_{wt}$ or
702 $C9_{TMH\text{-}1\ lock}$. d) OM damage was represented for all strains by the time when $DiOC_2$ influx
703 reached half the value of the peak ($t_{1/2peak}$, shown in a for $C9_{wt}$). e) IM damage was represented
704 for all strains by the time when Sytox fluorescence reached half the maximum value ($t_{1/2maximum}$,
705 shown in b for $C9_{wt}$). Multiwell plate-reader assays (a, b) are shown by one representative
706 experiment that has been repeated at least three times. Data represent mean +/- SD of three
707 independent experiments (c, d and e).

Figure 6 – Polymerization of C9 is impaired on complement-resistant *E. coli* strains

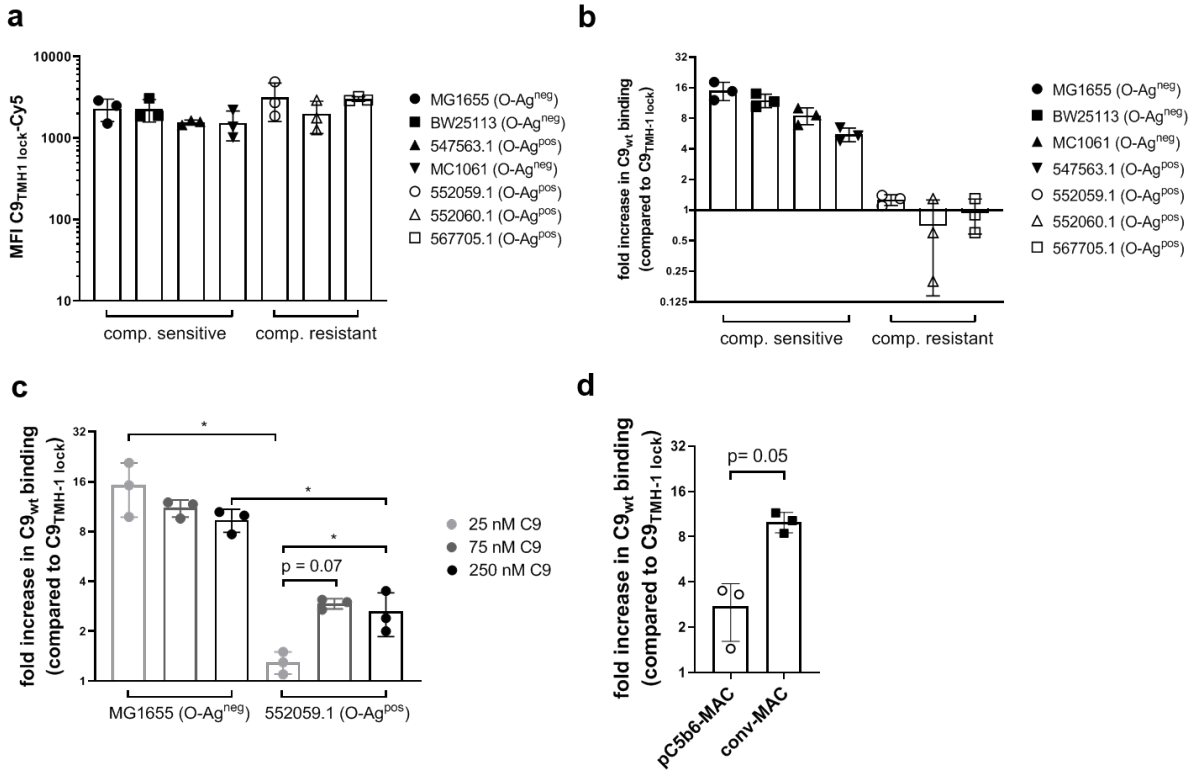

Complement-resistant (552059.1, 552060.1 and 567705.1) and complement-sensitive (MG1655, BW25113, MC1061 and 547563.1) *E. coli* strains were incubated in 3% C9-depleted serum supplemented with a physiological concentration (= 25 nM) of Cy5-labelled $C9_{wt}$ or $C9_{TMH\text{-}1\ lock}$ for 30 minutes to measure C9 binding by flow cytometry. a) Binding of Cy5-labelled $C9_{TMH\text{-}1\ lock}$ to bacteria. b) The relative increase in $C9_{wt}$ binding compared to bacteria labelled with $C9_{TMH\text{-}1\ lock}$ was calculated as indication for C9 polymerization. c) The relative increase in $C9_{wt}$ binding compared to bacteria labelled with $C9_{TMH\text{-}1\ lock}$ was compared for complement-sensitive MG1655 and complement-resistant 552059.1 at different C9 concentrations. d) MG1655 was labelled with convertases in 10% C5-depleted serum. Next, bacteria were washed and 3 nM of preassembled C5b6 (pC5b6) or C5 and C6 (conv-MAC) were added, together with excess 20 nM C7, 20 nM C8 and 50 nM Cy5-labelled $C9_{wt}$ or $C9_{TMH\text{-}1\ lock}$ for 30 minutes. The relative increase in $C9_{wt}$ binding compared to bacteria labelled with $C9_{TMH\text{-}1\ lock}$ was represented. Flow cytometry data are represented by MFI values of the bacterial population. Data represent individual values with mean +/- SD of three independent experiments. Statistical analysis was done on ^{2}log-transformed data (a, c, d) using a paired one-way ANOVA with Tukey's multiple comparisons' test. Significance was shown as * $p \leq 0.05$.

727 **Figure 7 – Assembly of complete MAC pores enhances OM damage and bacterial killing**

728

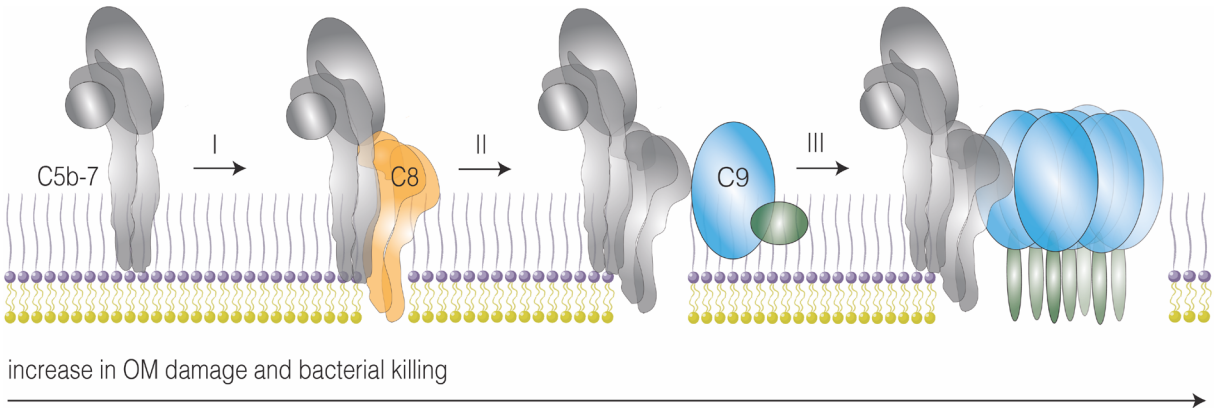

729

730

731 Schematic overview of the assembly of complete MAC pores. I) C8 (orange) binds to
732 membrane-anchored C5b-7 (grey) and subsequently inserts transmembrane β-hairpins into the
733 bacterial outer membrane (OM), which causes small lesions in the OM. II) Binding of C9 (blue)
734 to C5b-8 without polymerization of C9 slightly increases the OM damage and bacterial killing.
735 III) Polymerization of C9 forms a transmembrane polymeric-C9 ring, which drastically
736 increases OM damage and rapidly kills bacteria.